Electronic Supplementary Material (ESI) for MedChemComm.

Supporting Information

Structure-Based Virtual Screening for Fragment-Like Ligands of the G Protein-Coupled Histamine H_4 Receptor

Enade P. Istyastono,[‡ab] Albert J. Kooistra,[‡a] Henry F. Vischer,[a] Martien Kuijer,[a] Luc Roumen,[a] Saskia Nijmeijer,[a] Rogier A. Smits,[c] Iwan J.P. de Esch,[a] Rob Leurs[a] and Chris de Graaf[*a]

[a] Division of Medicinal Chemistry, Amsterdam Institute for Molecules, Medicines and Systems (AIMMS), Faculty of Exact Sciences, VU University Amsterdam, De Boelelaan 1083, 1081 HV Amsterdam - The Netherlands. E-mail: C.de.Graaf@vu.nl

[b] Center for Environmental Studies Sanata Dharma University (CESSDU) | Division of Drug Design and Discovery, Faculty of Pharmacy, Universitas Sanata Dharma, Depok, Sleman, Yogyakarta 55282 - Indonesia

[c] Griffin Discoveries B.V., De Boelelaan 1083, 1081 HV Amsterdam - The Netherlands

‡ These authors contributed equally.

Table of Contents:

Supplementary Fig. S1 Full sequence alignment of the H_4R homology models and the modeling templates (human β_2R and human H_1R)[a] showing the binding pocket residues for each model S2

Supplementary Fig. S2 Structure and biological activity of H_4R-active compounds discovered in a SBVS campaign by Kiss *et al.* (**4**-**7**) and by Vass *et al.* (**8**) with a $pK_i \geq 5$..... S3

Supplementary Fig. S3 Structure of the fragments selected in the β_2R-based prospective VS campaigns. S4

Supplementary Fig. S4 Structure of the fragments selected in the H_1R-based prospective VS campaigns. S5

Supplementary Fig. S5 Shared chemical similarity of the SBVS hits as determined by ECFP-4..... S6

Supplementary Fig. S6 Scatter-plots of the $PLANTS_{ChemPLP}$ scores versus the Tc-IFP scores for the fragment screening dataset (grey) with the inactive (blue) and the active hits (red) from β_2R-based SBVS-1, β_2R-based SBVS-2, H_1R-based SBVS-1, and H_1R-based SBVS-2. ..... S7

Supplementary Table S1 Vendors selected in the prospective SBVS campaigns. S8

Supplementary Table S2 The selected fragments from the β_2R-based prospective SBVS campaigns and related vendor information. S8

Supplementary Table S3 The selected fragments from the H_1R-based prospective SBVS campaigns and related vendor information. S9

Supplementary Table S4 Purity data for each of the validated compounds as measured by LC-MS S9

References S10

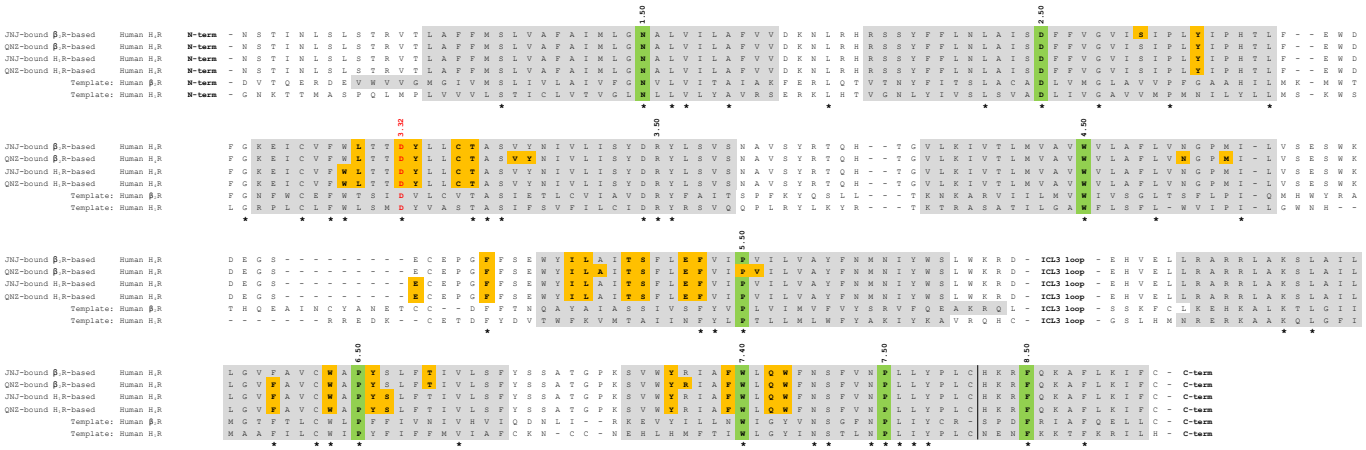

Supplementary Fig. S1. Full sequence alignment of the H_4R homology models and the modeling templates (human β_2R and human H_1R)[1] showing the binding pocket residues for each model (highlighted in orange).

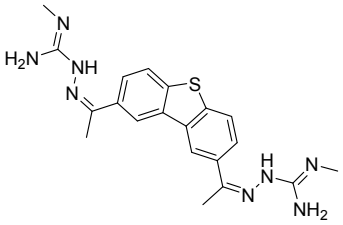

4; pK_i H_4R = 5.8

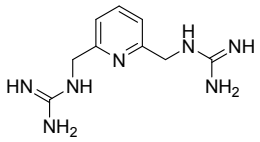

5a; pK_i H_4R = 5.9

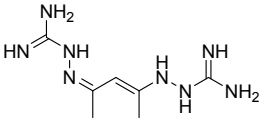

5b; pK_i H_4R = 6.0

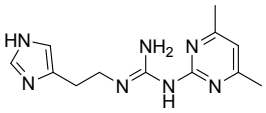

6; pK_i H_4R = 7.1

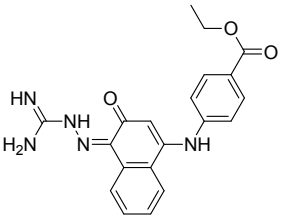

7; pK_i H_4R = 6.7

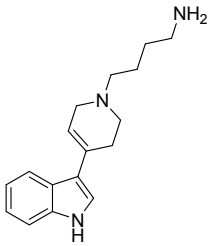

8; pK_i H_4R = 5.1

Supplementary Fig. S2 Structure and biological activity of H_4R-active compounds discovered in a SBVS campaign by Kiss *et al.* (**4**-**7**)[2] and by Vass *et al.* (**8**) with a pK_i ≥ 5.[3]

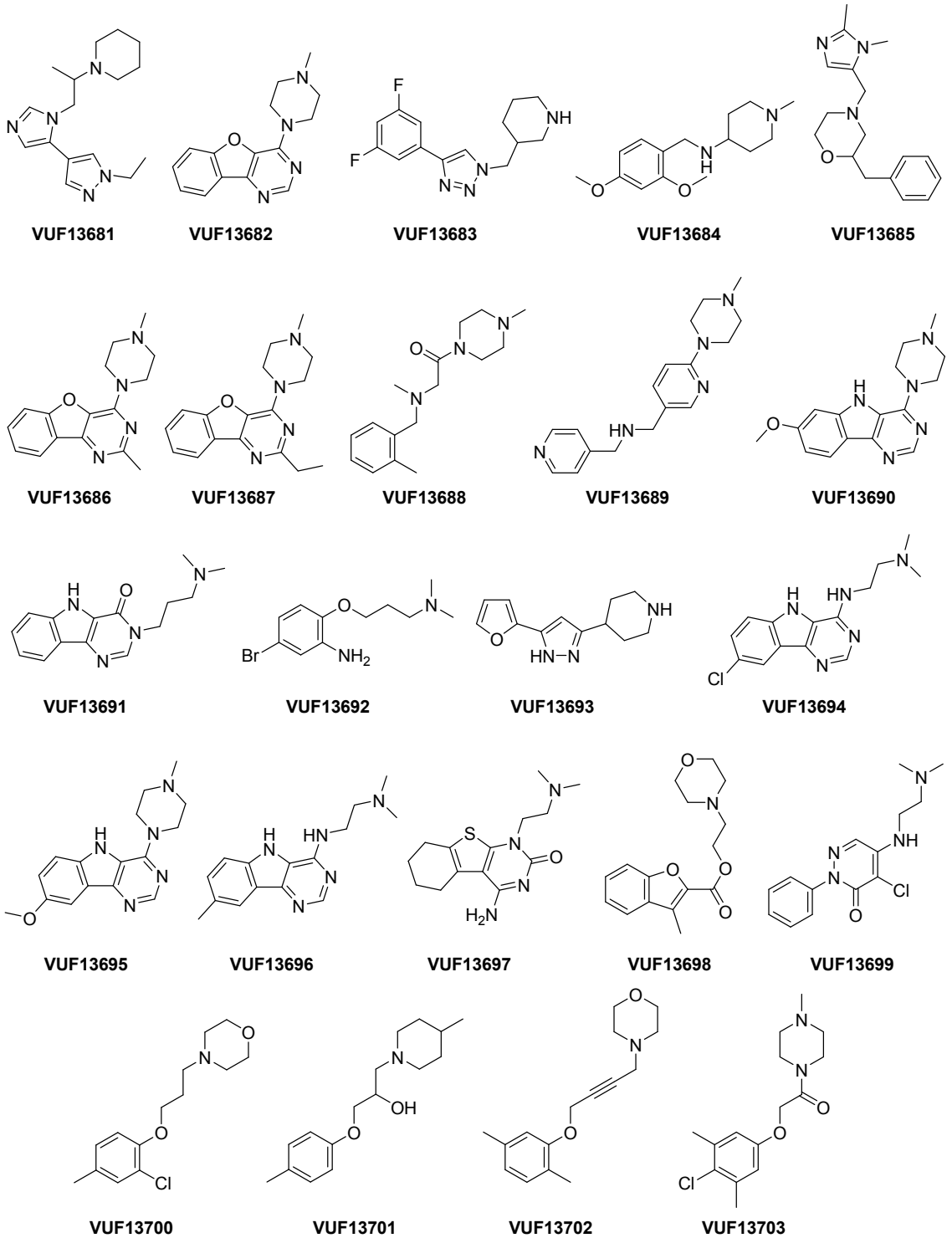

Supplementary Fig. S3 Structure of the fragments selected in the β_2R-based prospective VS campaigns.

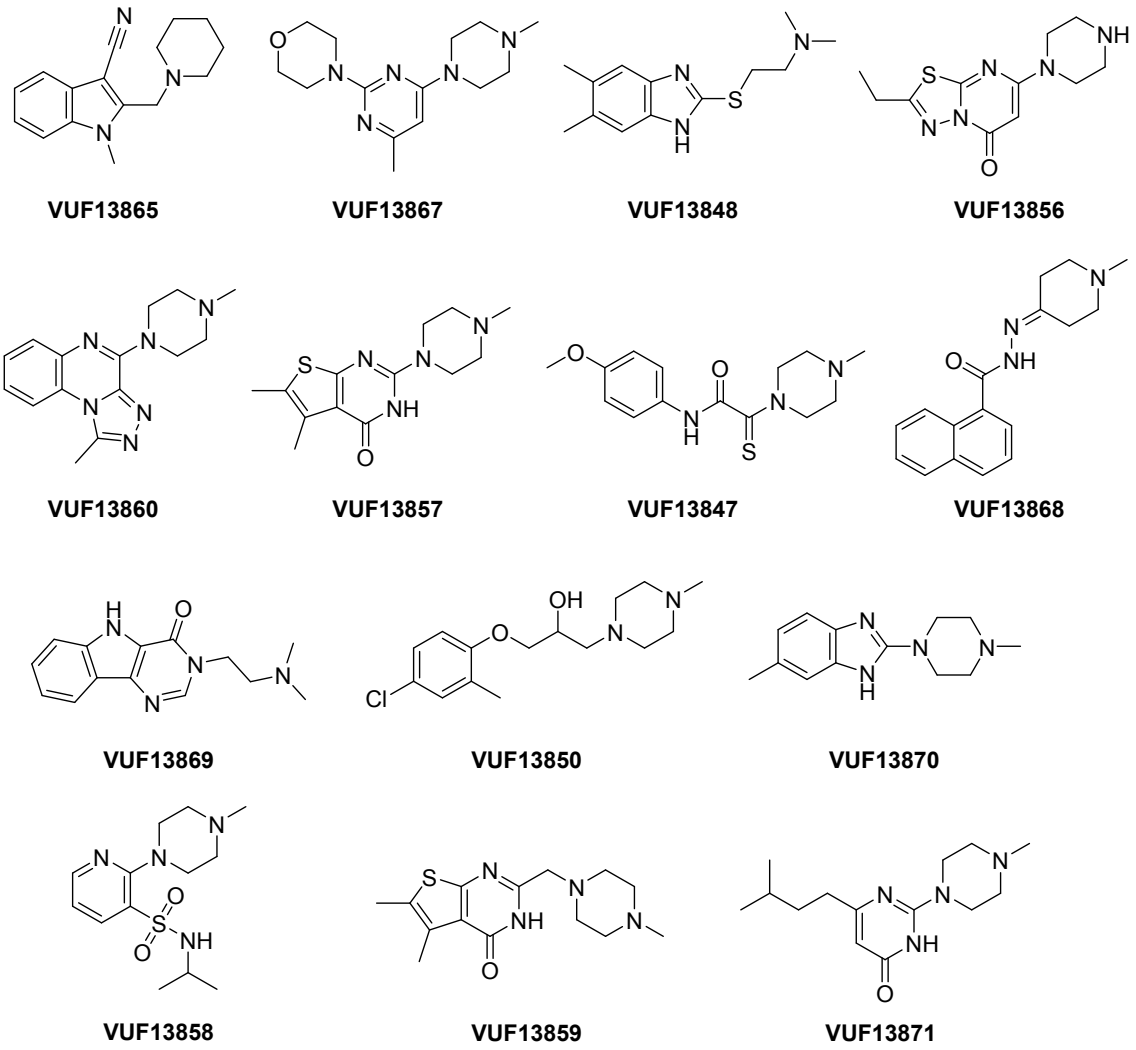

Supplementary Fig. S4 Structure of the fragments selected in the H_1R-based prospective VS campaigns.

	cpd 9a	cpd 9b	cpd 9c	cpd 10a	cpd 10b	cpd 10c	cpd 11	cpd 12	cpd 13
cpd 9a	1.00	0.70	0.67	0.41	0.16	0.41	0.06	0.33	0.28
cpd 9b	0.70	1.00	0.73	0.29	0.10	0.29	0.11	0.37	0.32
cpd 9c	0.67	0.73	1.00	0.29	0.11	0.29	0.09	0.32	0.28
cpd 10a	0.41	0.29	0.29	1.00	0.28	0.83	0.13	0.25	0.25
cpd 10b	0.16	0.10	0.11	0.28	1.00	0.34	0.25	0.10	0.10
cpd 10c	0.41	0.29	0.29	0.83	0.34	1.00	0.13	0.25	0.25
cpd 11	0.06	0.11	0.09	0.13	0.25	0.13	1.00	0.13	0.12
cpd 12	0.33	0.37	0.32	0.25	0.10	0.25	0.13	1.00	0.27
cpd 13	0.28	0.32	0.28	0.25	0.10	0.25	0.12	0.27	1.00

Supplementary Fig. S5. Shared chemical similarity of the SBVS hits as determined by ECFP-4.[4] This analysis highlights that the 9 SBVS hits cover 5 different scaffolds. Although compounds 10a/b/c share the same scaffold, compound 10b obtained a relatively low similarity score (when compared to compounds 10a/c) due to its linear linker.

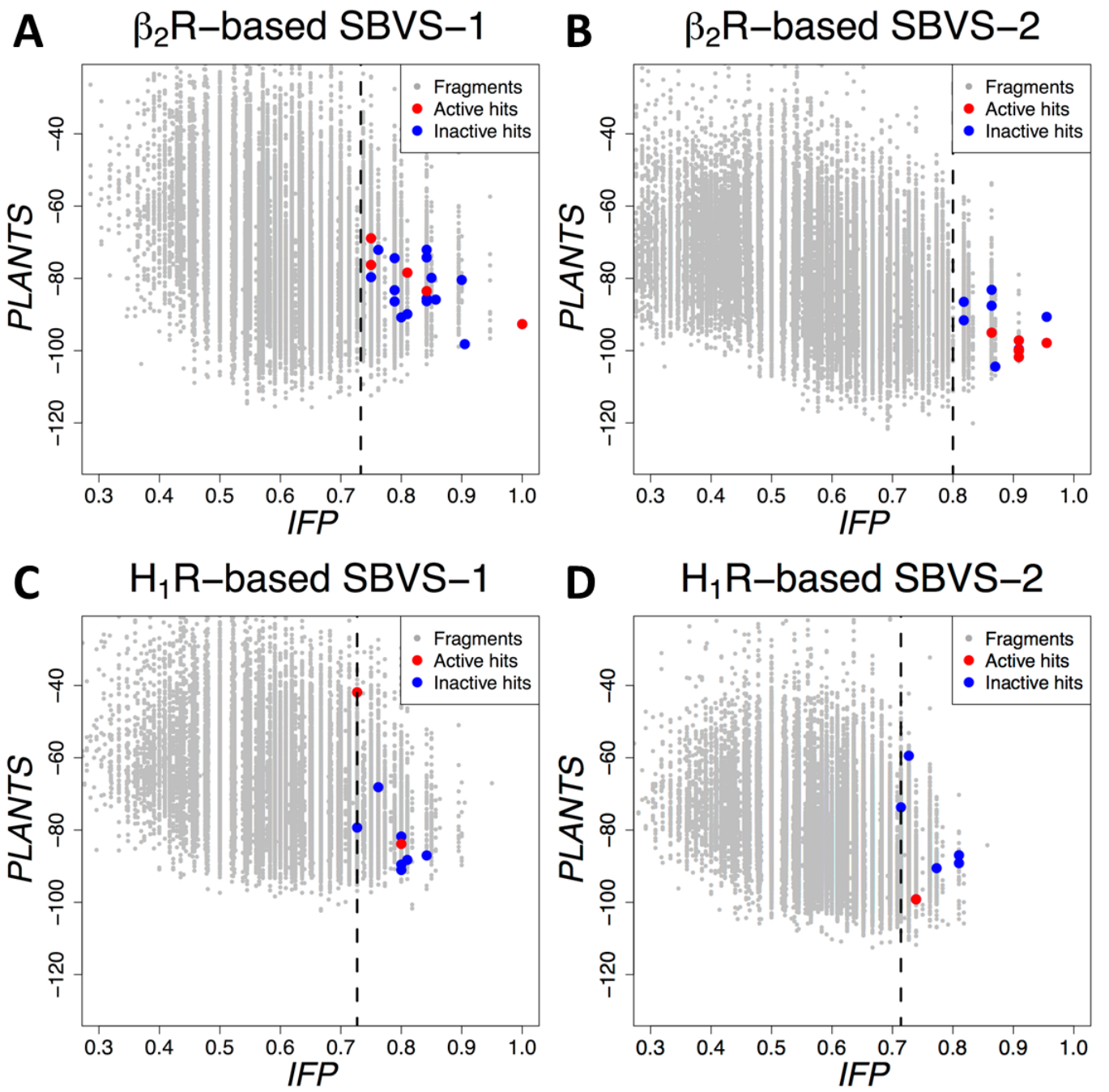

Fig. S6 Scatter-plots of the $PLANTS_{ChemPLP}$ scores (PLANTS) versus the Tc-IFP scores (IFP) for the fragment screening dataset (grey) with the inactive (blue) and the active hits (red) from β_2R-based SBVS-1 (A), β_2R-based SBVS-2 (B), H_1R-based SBVS-1 (C), and H_1R-based SBVS-2 (D). The dotted lines indicate the selected model cutoffs (Tc-IFP ≥ 0.733, 0.810, 0.727, and 0.714 for A, B, C, and D respectively).

Table S1 Vendors selected in the prospective SBVS campaigns.

Vendor	Website
Acros Organics	www.acros.be
Apollo Scientific	www.apolloscientific.co.uk
Asinex	www.asinex.com
ChemBridge	www.chembridge.com
Enamine	www.enamine.net
Fluorochem	www.fluorochem.co.uk
IBScreen	www.ibscreen.com
Labotest	www.labotest.com
Matrix Scientific	www.matrixscientific.com
Maybridge	www.maybridge.com
Sigma-Aldrich	www.sigma-aldrich.com
Specs	www.specs.net
TimTec	www.timtec.net
Vitas-M	www.vitasmlab.com

Table S2 The selected fragments from the β_2R-based prospective SBVS campaigns and related vendor information.

VUF code	ZINC code	Vendor	Vendor Code
VUF13681[a]	ZINC19719617	Asinex	SYN23712742
VUF13682[c]	ZINC03152027	Asinex	BAS01530286
VUF13683[c]	ZINC23506801	ChemBridge	82740504
VUF13684[a]	ZINC00182698	ChemBridge	5411809
VUF13685[b]	ZINC20541314	ChemBridge	86508374
VUF13686[a]	ZINC05141827	ChemBridge	9102853
VUF13687[a]	ZINC05216266	ChemBridge	9114126
VUF13688[b]	ZINC32819436	Enamine	T6368600
VUF13689[b]	ZINC30660859	Enamine	T6600538
VUF13690[a]	ZINC05025356	IBScreen	STOCK4S-01947
VUF13691[a]	ZINC00526020	IBScreen	STOCK1N-19344
VUF13692[a]	ZINC14630922	Matrix Scientific	22889
VUF13693[b]	ZINC04010314	TimTec	ST50950074
VUF13694[a]	ZINC05041012	Vitas-M	STK550071
VUF13695[a]	ZINC04834654	Vitas-M	STK530114
VUF13696[a]	ZINC05033346	Vitas-M	STK549702
VUF13697[c]	ZINC40268952	Vitas-M	STK935769
VUF13698[b]	ZINC00360026	Asinex	BAS00232858
VUF13699[b]	ZINC00118611	Asinex	BAS05154618
VUF13700[b]	ZINC04997152	ChemBridge	5539301
VUF13701[b]	ZINC05730526	ChemBridge	9116861
VUF13702[b]	ZINC16622482	ChemBridge	9117436
VUF13703[b]	ZINC04721959	ChemBridge	6107275

[a] Selected from the SBVS-1 and the SBVS-2. [b] Selected from the SBVS-1 only. [c] Selected from the SBVS-2 only.

Table S3 The selected fragments from the H_1R-based prospective SBVS campaigns and related vendor information.

VUF code	ZINC code	Vendor	Vendor Code
13865[c]	ZINC00049567	Vitas-M	STK024963
13867[c]	ZINC00073496	Vitas-M	STK537218
13848[b]	ZINC00191589	ChemBridge	5687092
13856[b]	ZINC00213538	Specs	AG-670/41935109
13860[b]	ZINC00236466	Vitas-M	STK538345
13857[a]	ZINC00388010	Specs	AR-434/42808028
13847[c]	ZINC02873245	ChemBridge	7950677
13868[b]	ZINC04719201	Vitas-M	STK445850
13869[c]	ZINC04808952	Vitas-M	STK529389
13850[b]	ZINC19781592	ChemBridge	5862214
13870[b]	ZINC19798275	Vitas-M	STK001495
13858[c]	ZINC19815505	Specs	AJ-333/25006070
13859[b]	ZINC19926650	Specs	AR-434/42808040
13871[b]	ZINC22448930	Vitas-M	STK871455

[a] Selected from the SBVS-1 and the SBVS-2. [b] Selected from the SBVS-1 only. [c] Selected from the SBVS-2 only.

Table S4 Purity data for each of the validated compounds as measured by LC-MS.[a]

Compounds	Purity (%)[a]
VUF13682 (**9a**)	100
VUF13686 (**9b**)	100
VUF13687 (**9c**)	95
VUF13690 (**10a**)	99
VUF13694 (**10b**)	96
VUF13695 (**10c**)	100
VUF13848 (**11**)	100
VUF13860 (**12**)	100
VUF13867 (**13**)	97

[a] Analytical HPLC-MS analyses were conducted using a Shimadzu LC-20AD liquid chromatograph pump system with a Shimadzu SPD-M20A diode array detector. MS detection was performed with a Shimadzu LCMS-2010 EV liquid chromatograph mass spectrometer. The analyses were performed using the following conditions; Xbridge (C18) 5 µm column (50 mm × 4.6 mm) with solvent A (acetonitrile with 0.1% formic acid) and B (water with 0.1% formic acid), flow rate of 1.0 mL/min, start 5% A, linear gradient to 90% A in 4.5 min, then 1.5 min at 90% A, then a linear gradient to 5% A in 0.5 min, then 1.5 min at 5% A, total run time of 8.0 min. Compound purities were calculated as the percentage peak area of the analyzed compound by UV detection at 230 nm.

References

1. A. J. Kooistra, S. Kuhne, I. J. de Esch, R. Leurs and C. de Graaf, *Br J Pharmacol*, 2013, **170**, 101-126.
2. R. Kiss, B. Kiss, A. Konczol, F. Szalai, I. Jelinek, V. Laszlo, B. Noszal, A. Falus and G. M. Keseru, *J Med Chem*, 2008, **51**, 3145-3153.
3. M. Vass, É. Schmidt, F. Horti and G. M. Keserű, *Eur. J Med Chem*, 2014, **77**, 38-46.
4. D. Rogers and M. Hahn, *J Chem Info Model*, 2010, **50**, 742-754.